

## Progresses on Reactions of Weakly Bound Nuclei at Near-barrier Energies

Z. J. Huang<sup>1</sup>, C. J. Lin<sup>1,2,\*</sup>, L. Yang<sup>1</sup>, H. M. Jia<sup>1</sup>, F. Yang<sup>1</sup>, N. R. Ma<sup>1</sup>, P. W. Wen<sup>1</sup>, T. P. Luo<sup>1</sup>, C. Chang<sup>1</sup>, H. R. Duan<sup>1</sup>, S. X. Zhu<sup>1</sup>, and C. Yin<sup>1</sup>

<sup>1</sup>China Institute of Atomic Energy, P. O. Box 275(10), Beijing 102413, China

<sup>2</sup>College of Physics and Technology & Guangxi Key Laboratory of Nuclear Physics and Technology, Guangxi Normal University, Guilin 541004, China

**Abstract.** Reactions of weakly bound stable and unstable nuclei have been extensively investigated for several decades. Unique structural effects and breakup mechanisms of weakly bound nuclei have consistently been focal points in the research of nuclear physics, especially at energies around the Coulomb barrier. This paper will review the recent experimental researches performed by the Nuclear Reaction Group at the China Institute of Atomic Energy on weakly bound nuclear reactions in the near-barrier energy region. An anomalous threshold phenomenon in the optical potentials of the  ${}^6\text{He} + {}^{208}\text{Bi}$  system has been observed. Results indicate that the dispersion relation cannot describe the relation between the real part and imaginary part of the optical potential. Moreover, breakup mechanisms of stable weakly bound nuclei  ${}^6,7\text{Li}$  as well as proton-rich nuclei  ${}^{17}\text{F}$  and  ${}^8\text{B}$  have been studied. The similarities and differences in breakup mechanisms and their effects are discussed.

### 1 Introduction

In recent years, with the improvement of the quality of radioactive beams and the upgrade of detection techniques, there has been a great interest in the study of nuclear reaction mechanisms induced by weakly bound nuclei in the Coulomb barrier energy region. It is widely known that the average binding energy per nucleon in a typical nucleus is about 8 MeV, forming a tightly bound nuclear structure. However, there also exist exotic nuclei where nucleons are weakly bound to each other, such as  ${}^6\text{Li}$  and  ${}^9\text{Be}$ , and their separation energy is generally less than 5 MeV (the separation energy of  ${}^6\text{Li}$  is 1.474 MeV and that of  ${}^9\text{Be}$  is 1.665 MeV). Accordingly, such nuclei are called weakly bound nuclei. Their weakly bound nature is of great importance for understanding nuclear structure [1–4], nuclear potential [5, 6], and reaction dynamics [7, 8]. The reaction mechanisms within the energy region of the Coulomb barrier for weakly bound nuclear systems are quite complex compared to tightly bound nuclei. An important feature of weakly bound nucleus-nucleus collisions is the high probability of breakup, which leads to the formation of many-body open quantum systems (OQSs). In collisions of weakly bound nuclei, the breakups and therefore couplings to continuum states have to be considered. Such coupling effects strongly influence the reaction dynamics, which is particularly significant in the energy region near the Coulomb barrier. Studying the breakup mechanism, especially in the energy region near the Coulomb barrier, contributes to a deeper understanding of the dynamics of OQS.

Furthermore, the characteristic of high breakup probability in weakly bound nuclei also have an impact on the energy dependence of their interaction optical potential (OP). It is widely recognized that for tightly bound nuclei in the energy region near the Coulomb barrier, as the incident energy decreases, there is a localized peak in the real part of the potential accompanying a rapid decrease in the imaginary part. This phenomenon is called "threshold anomaly" (TA) [9–11]. This situation may change for weakly bound nuclei. The breakup probability of these nuclei is still large at energies below the Coulomb barrier. Therefore, the net polarization potential in the scattering of weakly bound nuclei not only includes an attractive potential caused by the coupling of the elastic channel with inelastic excitation and other direct reactions, but also contains a repulsive potential due to the breakup process. The usual TA can still be observed if the attractive potential is dominant. However, if the repulsive potential predominates, an anomalous behavior will be observed for such systems [12–16]: as the incident energy decreases below the barrier, the depth of the imaginary potential will not decrease to zero quickly, but show an increasing trend. We refer to this phenomenon as the anomalous threshold anomaly (ATA). Additionally, the dispersion relation seems to be difficult to apply to the real and imaginary parts of the OP in weakly bound nuclei systems.

This article will briefly review the research achievements of the nuclear reaction group of the China Institute of Atomic Energy in the field of weakly bound nuclei reactions in the near-barrier energy region in recent years, from two aspects: the optical potential of weakly bound nuclear systems and the breakup mechanism of weakly bound nu-

\*e-mail: [cjlin@ciae.ac.cn](mailto:cjlin@ciae.ac.cn)

clei. Additionally, it will provide a future outlook for development directions.

## 2 Optical model potentials of weakly bound nuclear systems

The optical model potential (OMP) is extensively employed to describe the interaction of nuclear collisions. In general, OMPs are extracted by fitting angular distributions of elastic scattering. However, in the region of energies near and below the barrier, the angular distributions become featureless and it is difficult to obtain effective information. Therefore, we proposed an original method [17] for studying the OMPs of weakly bound nuclear systems by transfer reactions, which can yield fairly precise results. This method utilizes transfer reactions induced by stable nuclear beams as probes, extracting the OMP parameters of the system in the exit channel by fitting the angular distribution of the transfer reactions. The sensitivity of this method has been investigated theoretically [18], and the reliability was confirmed experimentally in the previous works [19, 20].

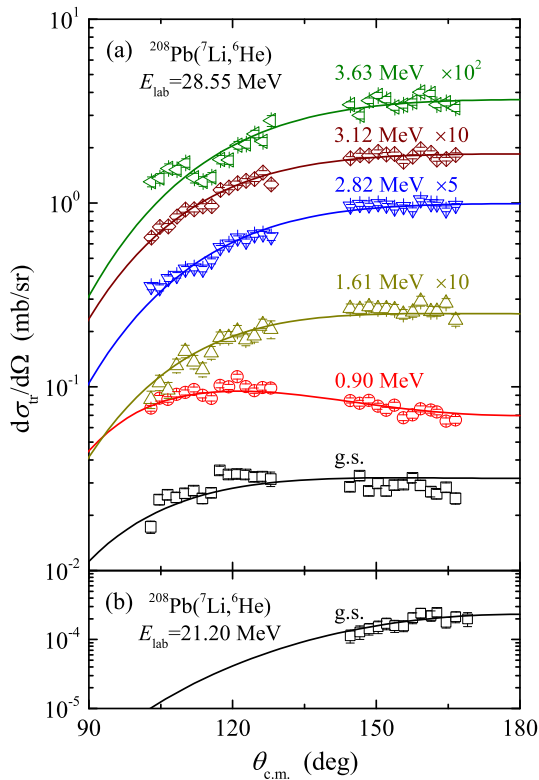


**Figure 1.** Angular distributions of  $^{208}\text{Pb}(^7\text{Li}, ^6\text{He})^{209}\text{Bi}$  reactions for proton transferred to different states of  $^{209}\text{Bi}$ . The figure is taken from [21].

Based on the transfer reaction method, for the first time, we have precisely determined the reaction threshold of the neutron halo nuclear system  $^6\text{He} + ^{208}\text{Bi}$  through the single-proton transfer reaction  $^{208}\text{Pb}(^7\text{Li}, ^6\text{He})^{209}\text{Bi}$ , clearly revealing the ATA phenomenon [19, 21]. Two experiments have been done at HI-13 tandem accelerator. Reaction energies in the laboratory frame were 21.20,

24.30, 25.67, and 28.55 MeV for the low-energy experiment, and were 42.55, 37.55, 32.55, 28.55, 25.67 MeV for the high-energy case. Angular distributions of transfer reactions at some typical energies are shown in Fig. 1. It can be seen that as the reaction energy decreases, the number of final excited states that can be confidently determined is reduced. At lower energies of 21.20 and 24.30 MeV, respectively, only the ground state and the first excited state of  $^{209}\text{Bi}$  resulting from the process of one proton transfer from  $^7\text{Li}$  to  $^{208}\text{Pb}$  could be observed. To extract the OMP parameters of the exit channel, the coupled reaction channels (CRC) approach was applied to fit the experimental data with the code FRESKO [22], and the fitting results are shown in Fig. 1 by the solid curves.

The energy dependencies of the real and imaginary potentials at the sensitivity radius 13.5 fm are shown in Fig. 2. As shown in this figure, a strong energy dependence is observed for both the real and imaginary potentials. For the real part, it exhibits a bell-shaped structure near the barrier ( $V_B \approx 20$  MeV in the center of mass system), which also can be observed in tightly bound nuclear systems. For the imaginary part, the strength increases first as the reaction energy decreases in the sub-barrier region. Such behavior is referred to as ATA. Moreover, in the deep sub-barrier region, the decreasing trend in the imaginary part is observed for the first time, and the threshold energy is determined as 13.73 MeV ( $\sim 0.68V_B$ ). The low threshold energy may be attributed to the extended matter distribution and small binding energy of the halo nucleus  $^6\text{He}$ .

Using the linear schematic model [11], we obtained the predicted curve for the dispersion relation, which are depicted with a red solid line in Fig. 2. Comparison with the experimental results clearly shows that the dispersion relation for  $^6\text{He} + ^{208}\text{Bi}$  does not hold true, which might be a common phenomenon in systems involving exotic nuclei [12, 13, 23]. The dispersion relation is derived from causality, hence the non-applicability of the dispersion relation is an extremely anomalous phenomenon. Although there have been some possible explanations for this anomaly [21, 24], further study is required to discover the underlying physics.

## 3 Breakups of weakly bound nuclei

### 3.1 Breakup reactions of stable nuclei: $^6,7\text{Li} + ^{209}\text{Bi}$

In many fusion experiments involving weakly bound stable nuclei, such as  $^6\text{Li}$  and  $^7\text{Li}$ , the complete fusion (CF) cross-section above the barrier energy obtained from the experiments is reduced by about 30% compared to the cross-section calculated by the coupled channels model. This suppression of CF is closely related to the appearance of incomplete fusion products [25–30]. Weakly bound nuclei have a lower breakup threshold, and they are more likely to break apart into fragments, which can then be absorbed by the target nucleus to form incomplete fusion products. So, this suggests that the CF suppression is caused by the breakup of weakly bound nuclei. In order for us to better understand the breakup effect of weakly bound nuclei on the suppression of complete fusion, our

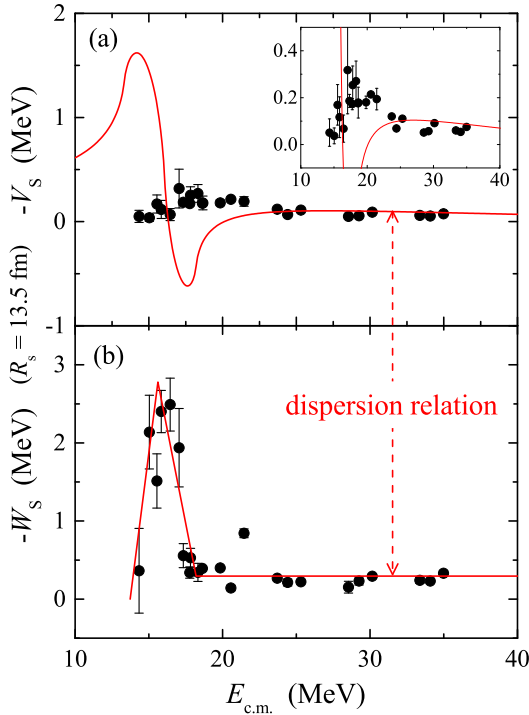


**Figure 2.** Energy dependence of the real (a) and imaginary (b) potentials at the sensitivity radius of 13.5 fm for the  ${}^6\text{He} + {}^{208}\text{Bi}$  system. the solid curve in (b) shows the fitting for the imaginary potential, and the prediction of the dispersion relation according to the variation of the imaginary potential is represented in (a) by the solid curve. The figure is taken from [21].

group conducted a detailed study of the relative probability of exclusive breakup channels in the  ${}^{6,7}\text{Li} + {}^{209}\text{Bi}$  reaction at energies around and above the Coulomb barrier (30, 40, and 47 MeV) [31]. Through the relative energies of the breakup fragments, different breakup components (prompt breakups and delayed breakups) and various breakup modes ( $\alpha + p$ ,  $\alpha + d$ ,  $\alpha + t$  and  $\alpha + \alpha$ ) are distinguished. The relative contributions of the observed breakup modes to the total breakup and prompt breakup respectively are shown in Fig. 3.

For reactions induced by  ${}^6\text{Li}$ , the contribution to the total breakup of direct breakup into  $\alpha + d$  is more significant than the  $\alpha + p$  breakup following  $1n$ -stripping. Moreover, the breakup channel  $\alpha + p$ , rather than the  $\alpha + d$  process, becomes the main contributor to the total prompt breakup cross section. For reactions induced by  ${}^7\text{Li}$ , the main contribution to the total breakup cross section is due to the  $\alpha + \alpha$  breakup of  ${}^8\text{Be}$ , which is induced by the  $1p$  pick-up reaction. For prompt breakup, it can be observed that  $\alpha + \alpha$  breakup is the major contributor, and it becomes more significant with the increasing bombarding energy. As shown in Fig. 4 are the relative probabilities of prompt and delayed breakup for the  ${}^{6,7}\text{Li}$  reactions on  ${}^{209}\text{Bi}$  under different modes. Delayed breakup plays a minor role in the  $\alpha + \alpha$  and  $\alpha + t$  breakup modes for  ${}^6\text{Li}$  and  ${}^7\text{Li}$ , respectively. However, for the  $\alpha + d$  channel, due to the presence of a long-lived  $3^+$  resonant state in  ${}^6\text{Li}$ , the

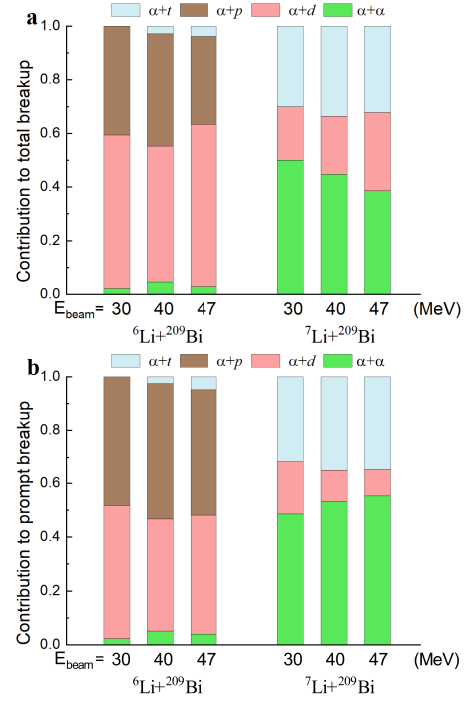


**Figure 3.** Relative contributions to (a) the total and (b) the total prompt breakup of various breakup modes of  ${}^{6,7}\text{Li}$  on  ${}^{209}\text{Bi}$  at 30, 40 and 47 MeV. The figures are taken from [31].

importance of delayed breakup increases with increasing incident energy.

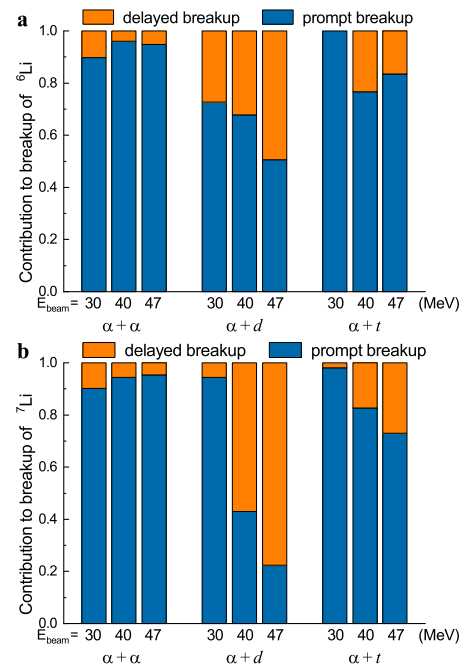


**Figure 4.** Relative contributions of various breakup modes of  ${}^{6,7}\text{Li} + {}^{209}\text{Bi}$ . The histograms show the prompt and the delayed breakup to the total breakup of  ${}^{6,7}\text{Li} + {}^{209}\text{Bi}$  at indicated energies. The figures are taken from [31].

Through this work, rich information on breakups of  ${}^{6,7}\text{Li}+{}^{209}\text{Bi}$  was obtained experimentally, which requires a unified theory to comprehensively understand the dynamics and its influences.

### 3.2 Breakup reactions of proton-rich nuclei: ${}^{17}\text{F} + {}^{58}\text{Ni}, {}^8\text{B} + {}^{120}\text{Sn}$

For proton-rich nuclei, there are currently only a few experimental research results available. Therefore, the reaction mechanism of proton-rich nuclei in the near-barrier energy region is an unexplored blank area that urgently needs to be investigated. Currently, the research mainly focuses on the two nuclei,  ${}^8\text{B}$  and  ${}^{17}\text{F}$ . We have conducted full kinematic measurements for these two proton-drip nuclei at the Center for Nuclear Study Radioactive Ion Beam separator (CRIB) at the University of Tokyo, Japan [32–34].

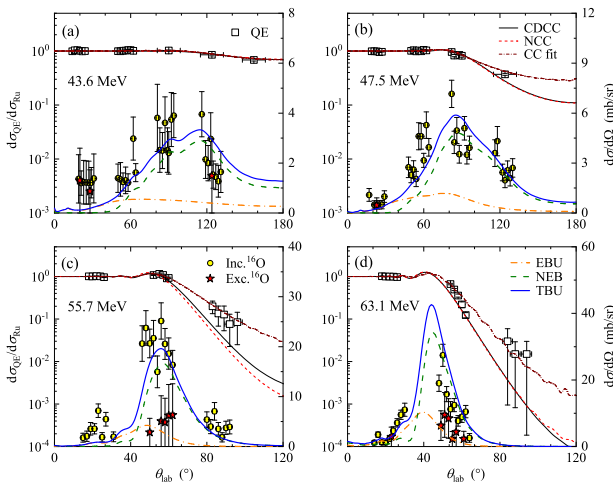


**Figure 5.** Angular distributions of quasi-elastic scattering (open squares), exclusive (stars) and inclusive (solid circles) breakup reactions of  ${}^{17}\text{F}+{}^{58}\text{Ni}$  at 43.6 MeV (a), 47.5 MeV (b), 55.7 MeV (c) and 63.1 MeV (d). The thin solid, dashed and dotted-dashed curves represent the CDCC calculations, CDCC calculations without the couplings from the continuum states and coupled channel fitting results. The thick dotted-dashed and dashed curves denote the CDCC and IAV calculation results, which are responsible for the EBU and NEB. The thick solid curve is the sum of EBU and NEB results, i.e., the TBU. The results are taken from [33].

Measurements have been carried out for the  ${}^{17}\text{F}+{}^{58}\text{Ni}$  system at four energy points in the near-barrier energy region, 43.6 MeV, 47.5 MeV, 55.7 MeV, and 63.1 MeV. For the first time, complete identification of reaction products in the near-barrier energy region for the  ${}^{17}\text{F}$  interacting with a light target nucleus has been achieved, allowing the extraction of almost complete reaction channel information, such as the quasi-elastic scattering angular distribution, breakup reaction angular distribution, and total fusion reaction excitation function. The quasi-elastic scattering angular distribution, exclusive and inclusive breakup angular distributions obtained from the experiment are shown in Fig. 5. For quasi-elastic scattering, the results

from the continuum discretized coupled-channels (CDCC) method and the calculation without considering the coupling to continuum states are shown by the solid and dashed lines, respectively, in Fig. 5. For elastic breakup (EBU) and non-elastic breakup (NEB) angular distributions, calculations were performed using the CDCC and Ichimura, Austern and Vincent (IAV) model [35], with the results shown by the bold dashed and dot-dash lines in Fig. 5. The sum of these two represents the total breakup (TBU) process, corresponding to the inclusive measurement, i.e., the inclusive breakup result. It can be seen that the theoretical EBU and TBU are able to reproduce the exclusive and inclusive experimental data quite well. Moreover, within the measured energy range, NEB is the dominant breakup process.

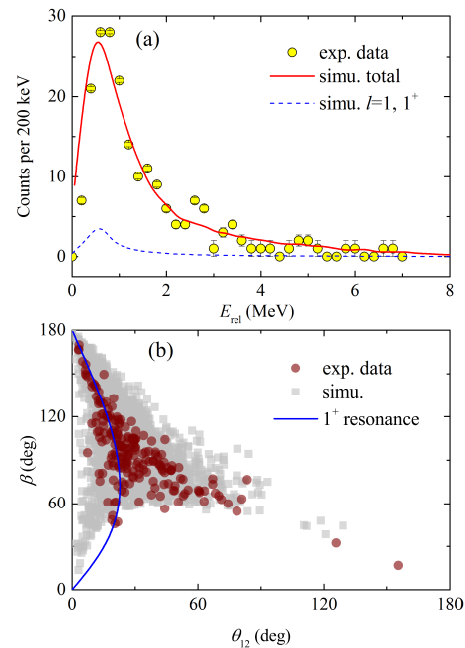


**Figure 6.** Measured relative energy ( $E_{rel}$ ) distribution (a) and angular correlation (b) for breakup fragments  ${}^7\text{Be}$  and  $p$  from the  ${}^8\text{B}+{}^{120}\text{Sn}$  system at 38.7 MeV: circles denote the experimental data, the solid and dashed curves in panel (a) represent the simulated distributions of  $E_{rel}$  and the contribution of the p-wave  $1^+$  state; the squares in panel (b) show the simulation results, and the solid curve denotes the expected  $\beta - \theta_{12}$  correlation assuming asymptotic breakup from the  $1^+$  resonance of  ${}^8\text{B}$ . The figures are taken from [32].

For the proton-halo nucleus  ${}^8\text{B}+{}^{120}\text{Sn}$  system, measurements were carried out at two energies of 38.7 MeV and 46.1 MeV near the barrier [34]. For the first time, the correlation between the proton-halo nucleus  ${}^8\text{B}$  breakup fragments has been derived. The breakup angular distribution indicates that the EBU is the primary mechanism for producing  ${}^7\text{Be}$ , providing exact evidence that the breakup is the main direct reaction process. Moreover, through the energy and angle correlations between the breakup fragments (Fig. 6), the complete breakup process has been reconstructed. In terms of data analysis, based on the CDCC combined with the Markov Chain Monte Carlo method, the microscopic description of the breakup and the contin-

uum state coupling effects has been achieved. The results show that: The breakup of  ${}^8\text{B}$  via the  $1^+$  resonant state accounts for only 4% of the total breakup cross section; the breakup of  ${}^8\text{B}$  is primarily a prompt process occurring in the outgoing trajectory.

## 4 Summary and outlook

We introduced the recent researches of the nuclear reaction group at the China Institute of Atomic Energy on weakly bound nuclear reactions. For the study of nuclear interaction, the anomalous threshold behavior in the  ${}^6\text{He}+{}^{209}\text{Bi}$  system was observed, where the dispersion relation is not applicable. Additionally, the researches on the breakup mechanisms of stable nuclei  ${}^6\text{Li}$  and  ${}^7\text{Li}$ , as well as proton-drip nuclei  ${}^8\text{B}$  and  ${}^{17}\text{F}$ , were also reviewed. Furthermore, we continue to expand and delve deeper into the existing research content, such as the optical potential study of the  ${}^6\text{Li}+{}^{208}\text{Pb}$  system in the deep sub-barrier and the breakup mechanisms of  ${}^7\text{Be}$ . These studies will provide valuable opportunities for a systematic and comprehensive understanding of the reaction dynamics of weakly bound nuclei and promote the development of nuclear reaction theory. Without a doubt, more systems with exotic nuclei are required to understand the dynamics of open quantum systems.

## References

- [1] I. Tanihata, H. Savajols, R. Kanungod, Prog. Part. Nucl. Phys. **68**, 215 (2013).
- [2] T. Frederico, A. Delfino, L. Tomiob, et al., Prog. Part. Nucl. Phys. **67** (4) 939 (2012).
- [3] T. Nakamura, Y. Kondo, *Clusters in Nuclei, Vol.2* (Springer Berlin Heidelberg, Berlin Heidelberg, 2012) 67.
- [4] W. Nazarewicz, J. Phys. G **43**, 044002 (2016).
- [5] N. Keeley, R. Raabe, N. Alamanos, et al., Prog. Part. Nucl. Phys. **59** (2) 579 (2007).
- [6] N. Keeley, N. Alamanos, K.W. Kemper, K. Rusek, Prog. Part. Nucl. Phys. **69**, 396 (2009).
- [7] N. Keeley, N. Alamanos, K.W. Kemper, et al., Prog. Part. Nucl. Phys. **63** (2) 396 (2009).
- [8] L. F. Canto, P.R.S. Gomes, R. Donangelo, M. S. Hussein, Phys. Rep. **424**, 1 (2006).
- [9] B. R. Fulton, D. W. Banes, J. S. Lilley et al., Phys. Lett. B **162**, 55 (1985).
- [10] G. R. Satchler, Phys. Rep. **199**, 147 (1991).
- [11] C. Mahaux, H. NGô, G. Satchler, Nucl. Phys. A **449**(2), 354 (1986).
- [12] A. Pakou, N. Alamanos, A. Lagoyannis et al., Phys. Lett. B **556**, 21 (2003).
- [13] A. Pakou, N. Alamanos, G. Doukelis et al., Phys. Rev. C **69**, 054602 (2004).
- [14] N. Keeley, S. J. Bennett, N. M. Clarke et al., Nucl. Phys. A **571**, 326 (1994).
- [15] Hussein M. S., Gomes P. R. S., Lubian J., et al., Phys. Rev. C **73**(4), 044610 (2006).
- [16] Niello J. O. F., Figueira J. M., Abriola D., et al., Nucl. Phys. A **787**(1-4), 484 (2007).
- [17] C. J. Lin, F. Yang, P. Zhou, H. Q. Zhang, Z. H. Liu, M. Ruan, X. K. Wu, and C. L. Zhang, AIP Conf. Proc. **853**, 81 (2006).
- [18] Wu Zhen-Dong, Yang Lei, Lin Cheng-Jian et al., Chin. Phys. Lett. **31**, 092401 (2014).
- [19] L. Yang, C. J. Lin, H. M. Jia et al., Phys. Rev. C **89**, 044615 (2014).
- [20] L. Yang, C. J. Lin, H. M. Jia et al., Phys. Rev. C **95**, 034616 (2017).
- [21] L. Yang, C. J. Lin, H.M. Jia et al., Phys. Rev. Lett. **119**, 042503 (2017).
- [22] I. J. Thompson, Computer Physics Reports **7**, 167 (1988).
- [23] R. Lipperheide, A. K. Schmidt, Nucl. Phys. A **112**, 65 (1968).
- [24] P. Kinsler, M. W. McCall, Phys. Rev. Lett. **101**, 167401 (2008).
- [25] N. T. Zhang, Y. D. Fang, P. R. S. Gomes, et al., Phys. Rev. C **90**, 024621 (2014).
- [26] Jin Lei, Antonio M. Moro, Phys. Rev. Lett. **122**, 042503 (2019).
- [27] M. Dasgupta, et al., Phys. Rev. Lett. **82**, 1395 (1999).
- [28] A. Mukherjee, et al., Phys. Lett. B **636**, 91 (2006).
- [29] L. F. Canto, P. Gomes, R. Donangelo, J. Lubian, M. Hussein, Phys. Rep. **596**, 1 (2015).
- [30] Y. D. Fang, P. R. S. Gomes, J. Lubian, et al., Phys. Rev. C **91**, 014608 (2015).
- [31] D. H. Luong, M. Dasgupta, D. J. Hinde, et al., Phys. Lett. B **695** (1-4), 105 (2011).
- [32] L. Yang, C. J. Lin, N. R. Ma, et al., Science Bulletin **68**(8), 775 (2023).
- [33] L. Yang, C. J. Lin, H. Yamaguchi, et al., Phys. Lett. B **813**, 136045 (2021).
- [34] L. Yang, C. J. Lin, H. Yamaguchi, et al., Nature Communications **13**, 7193 (2022).
- [35] M. Ichimura, N. Austern, C. M. Vincent, Phys. Rev. C **32**, 431 (1985).